

Full length article

Effect of Fe doping and magnetic field on martensitic transformation of Mn-Ni(Fe)-Sn metamagnetic shape memory alloys

P. Lázpita ^{a, b, *}, M. Sasmaz ^c, J.M. Barandiarán ^{a, b}, V.A. Chernenko ^{a, b, d}^a University of Basque Country (UPV/EHU), 48940, Leioa, Spain^b BCMaterials, 48940, Leioa, Spain^c Adiyaman University, 02040, Adiyaman, Turkey^d Ikerbasque, Basque Foundation for Science, 48013, Bilbao, Spain

ARTICLE INFO

Article history:

Received 1 December 2017

Received in revised form

13 April 2018

Accepted 22 May 2018

Available online 26 May 2018

Keywords:

Magnetic shape memory alloy
Martensitic phase transformation
Magnetic properties
Magnetostrain
Metamagnetic effect

ABSTRACT

In this work we report the elaboration of a family of metamagnetic shape memory alloys with composition $\text{Mn}_{49}\text{Ni}_{42-x}\text{Fe}_x\text{Sn}_9$ ($x = 0, 2, 3, 4, 5$ and 6 at.%) and the systematic study of their structure, martensitic transformation (MT) behavior and functional characteristics as a function of the Fe doping and magnetic field, up to 12 T. Regarding the influence of the magnetic field, we have tentatively divided the alloys into two groups: group I, alloys with $x = 0, 2, 3$ and 4 and group II, alloys with $x = 5$ and 6 . Group II alloys exhibit an appreciable amount of dispersed γ -phase and a field-induced arrest of MT. The alloys from group I show a large magnetization drop at MT that proceeds steeply. This group also displays a monotonous evolution of all studied properties with pronounced metamagnetic effect and large magnetostrain effect, reaching 0.3% , in the alloy with $x = 4$.

© 2018 Acta Materialia Inc. Published by Elsevier Ltd. All rights reserved.

1. Introduction

Heusler Ni-Mn-X ($X = \text{In}, \text{Sn}, \text{Sb}$) metamagnetic shape memory alloys (MetaMSMAs) have been extensively studied during the last decade due to their remarkable physical properties and large functional response associated to a first order martensitic transformation (MT) [1–3]. The strong magnetovolume coupling and concurrent ferromagnetic – antiferromagnetic interactions present in these compounds allow to control MT by means of magnetic field or pressure resulting in different multifunctional properties such as the giant inverse caloric effects (magnetocaloric, elastocaloric or barocaloric) [4–7], very large magnetoresistance [8,9] and the metamagnetic shape memory effect [1,10,11]. All these unusual effects open up novel possibilities for technical applications.

The magnetic driving force responsible of the metamagnetic transformation depends directly on the difference of magnetization value between the austenitic and martensitic phases at the MT. According to the Clausius-Clapeyron relationship:

$$-dT_M/d(\mu_0H) = \Delta M/\Delta S$$

(where μ_0H is the external applied magnetic field, T_M is the martensitic transformation temperature, ΔM and ΔS are the magnetization and entropy change at MT, respectively) a large ΔM together with a reduced ΔS are necessary to facilitate a field-induced MT. Besides, MT with low hysteresis width near room temperature is desired for high performance [12,13]. While tuning ΔS is hardly possible, ΔM and T_M can be tailored by modifying the composition and doping [14–16].

It is well-known that in the magnetic shape memory Heuslers the magnetization depends mainly on the magnetic moment on Mn atoms and their exchange interactions, which depend on the Mn-Mn interatomic distances [17–20]. So, increasing Mn content is promising to enhance the ΔM value in these compounds. In fact, systematic studies of Mn-based $\text{Mn}_{50}\text{Ni}_{50-x}\text{In}_x$ alloys reported by Xiang et al. [21] verified the possibility to develop the two-way magnetic field induced MT for $9 < x < 11$ compounds, due to their low hysteresis of MT and high ΔM (6 K and $60 \text{ Am}^2\text{kg}^{-1}$, respectively, for $x = 10$). Thus, these alloys present remarkable functionalities that make them competitive candidates for technical applications [21,22].

Mn-Mn exchange interactions can be affected also by the doping

* Corresponding author. University of Basque Country (UPV/EHU), 48940, Leioa, Spain.

E-mail address: patricia.lazpita@ehu.es (P. Lázpita).

with a fourth element. Specifically, doping with transition metals, like Co or Fe, promotes the ferromagnetic (FM) coupling of the nearest neighbors Mn atoms in the austenitic phase raising the magnetization saturation of this phase whereby triggering enhancement of ΔM at MT. In the case of the $\text{Mn}_{50}\text{Ni}_{40}\text{In}_{10}$ alloys, a 3 at.%Co addition increases ΔM from $40 \text{ Am}^2\text{kg}^{-1}$ [23,24] to $89 \text{ Am}^2\text{kg}^{-1}$ [25]. This doping also promotes the formation of secondary phases which improve the mechanical properties of these materials, in particular they mitigate the intrinsic brittleness of the MetaMSMAs [15,26,27].

In the present work, we perform a systematic study of the effect of Fe addition and applied magnetic field on MT and related functional properties in a series of the polycrystalline MetaMSMAs with a composition of $\text{Mn}_{49}\text{Ni}_{42-x}\text{Fe}_x\text{Sn}_9$ ($x = 0, 2, 3, 4, 5$). Particularly, we report the influence of the Ni substitution by Fe on MT, structure and microstructure, transformation characteristic temperatures and magnetization change at the transformation. The spontaneous strain accompanying MT has been also investigated, providing new details about the mechanism of the magnetic field induced strain effect observed in these alloys.

2. Experimental procedure

Polycrystalline ingots of $\text{Mn}_{49}\text{Ni}_{42-x}\text{Fe}_x\text{Sn}_9$ with $x = 0, 2, 3, 4, 5$ and 6 were prepared by induction melting of high purity metals (>99.9%) and then heat treated at 1173 K during 3 days under argon atmosphere for homogenization. Small pieces were cut from ingots and heat treated during 0.5 h at 1173 K with subsequent water quenching. After the heat treatment, the samples were mechanically polished to examine their microstructure by secondary electron imaging in a Hitachi TM300 table-top scanning electron microscope (SEM), also equipped with the energy dispersive X-ray (EDX) analysis. The compositions of the alloys were determined by EDX with an uncertainty of about 1 at. %. The results show a roughly good agreement between the measured averaged compositions and the nominal ones (Table 1). Obviously, the precipitation causes composition gradients in the alloys and an essential composition deviation in the transforming phase from the averaged one. All of these can influence the results due to a strong sensitivity of the MT to the composition variation. Therefore, some dispersion of results occurs for the parameters measured. Like in the case of $\text{Ni}_{50-x}\text{Fe}_x\text{Mn}_{39}\text{Sn}_{11}$ alloys [28], the MT characteristics were plotted as a function of nominal content of Fe to find out the general trends of Fe influence.

Diffraction patterns were collected at room temperature by a Bruker D8 Advance diffractometer with Cu $K\alpha$ radiation.

MT temperatures were obtained by means of differential scanning calorimetry curves (DSC Mettler Toledo 822e) measured at heating/cooling rate of 5 K/min. Thermomagnetic and magnetization loops measurements were carried out in a vibrating sample magnetometer (VSM) from Cryogenic Ltd. in a range of

temperatures between 10 K and 320 K, under applied magnetic fields up to 12 T. A home-made VSM was used for the temperatures from 300 K to 450 K at magnetic fields up to 1.8 T.

Magnetostrain measurements were performed with samples of $3.0 \text{ mm} \times 2.0 \text{ mm} \times 1.5 \text{ mm}$ using two strain gauges; one was glued on the sample and the other one on a quartz plate used as a reference. The strain parallel to the applied magnetic field was measured as a function of temperature between 150 K and 320 K and magnetic fields up to 12 T using a magnetic platform of Cryogenic Ltd.

3. Results and discussion

3.1. Crystal structure and microstructure

X-ray diffraction patterns of the bulk samples, depicted in Fig. 1,

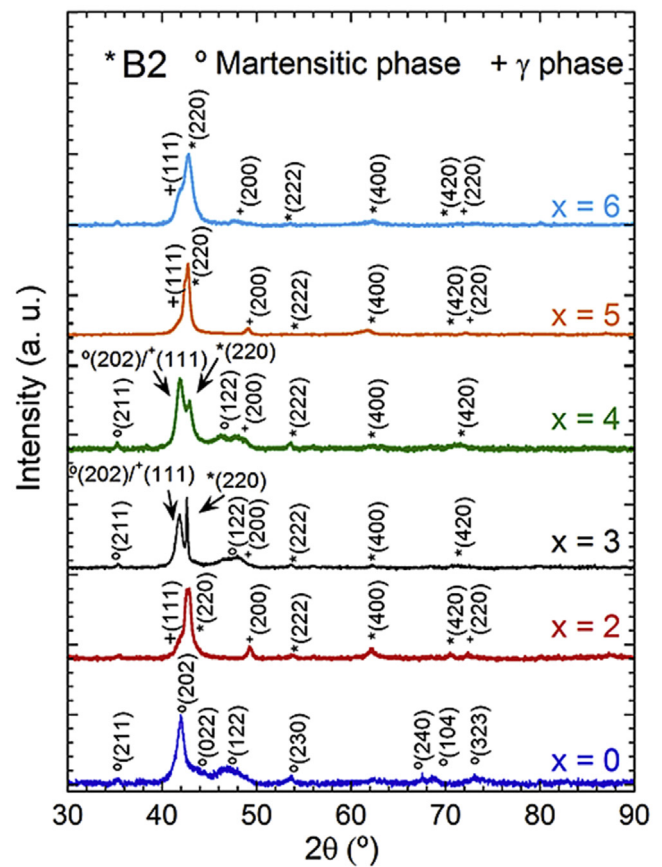


Fig. 1. X-ray diffraction patterns measured at room temperature for $\text{Mn}_{49}\text{Ni}_{42-x}\text{Fe}_x\text{Sn}_9$ with $x = 0, 2, 3, 4, 5$ and 6.

Table 1

Compositions of the $\text{Mn}_{49}\text{Ni}_{42-x}\text{Fe}_x\text{Sn}_9$ (at.%) alloys as determined by EDX. The compositions of matrix and γ -phase and volume fraction of latter are given separately. The average composition of the alloy is determined from the percentage of each element in both phases taking into account the volume fraction of γ -phase. Cell parameters are determined by X-ray diffraction in the austenite phase for the matrix and γ -phase, respectively.

Alloy	Matrix				γ -phase				γ -phase (vol.%)	Average composition				Cell parameter (Å)	
	Mn	Ni	Sn	Fe	Mn	Ni	Sn	Fe		Mn	Ni	Sn	Fe	Matrix	γ -phase
x = 0	44.8	45.9	9.3	–	–	–	–	–	0.0	44.8	45.9	9.3	0.0	–	–
x = 2	49.5	39.3	9.7	1.5	63.2	28.9	2.9	5.1	1.1	49.7	39.2	9.6	1.5	6.00	–
x = 3	47.1	41.3	10.5	1.1	61.3	29.7	6.7	2.3	9.2	48.4	40.2	10.2	1.2	6.02	3.74
x = 4	48.1	40.0	9.6	2.4	59.4	30.4	3.1	7.1	13.3	49.6	38.7	8.7	3.0	6.01	3.73
x = 5	45.7	40.9	10.6	2.8	53.6	33.4	3.2	9.7	19.1	47.2	39.5	9.2	4.1	5.99	3.74
x = 6	46.9	39.2	10.6	3.3	58.1	29.1	2.9	9.8	30.0	50.3	36.2	8.3	5.3	6.02	3.74

Download English Version:

<https://daneshyari.com/en/article/7875366>

Download Persian Version:

<https://daneshyari.com/article/7875366>

[Daneshyari.com](https://daneshyari.com)